Molecular dynamics study of self-diffusion in bcc Fe

Mikhail I. Mendelev*
Materials and Engineering Physics, Ames Laboratory, Ames, Iowa 50011, USA

Yuri Mishin
Department of Physics, MSN 3F3, George Mason University, Fairfax, Virginia 22030, USA
(Received 19 May 2009; revised manuscript received 7 July 2009; published 26 October 2009)

A semiempirical interatomic potential for Fe was used to calculate the diffusivity in bcc Fe assuming the vacancy and interstitial mechanisms of self-diffusion. Point-defect concentrations and diffusivities were obtained *directly* from molecular dynamics (MD) simulations. It was found that self-diffusion in bcc Fe is controlled by the vacancy mechanism at all temperatures. This result is due to the fact that the equilibrium vacancy concentration is always much larger than the equilibrium interstitial concentration. The predominance of the equilibrium vacancy concentration over the interstitial concentration is explained by the lower vacancy-formation energy at low temperatures and high vacancy-formation entropy at high temperatures. The calculated diffusivity is in good agreement with experimental data. The MD simulations were also used to test the quasiharmonic (QH) approximation for point-defect calculations. It was found that the QH approximation can considerably underestimate variations in point-defect characteristics with temperature.

DOI: 10.1103/PhysRevB.80.144111 PACS number(s): 66.30.Fq, 02.70.Ns, 61.72.jd, 61.72.jj

I. INTRODUCTION

Diffusion plays an important role in the kinetics of many materials processes.[1] Experimental measurements of diffusion coefficients are expensive, difficult and in some cases nearly impossible. A complimentary approach is to determine diffusivities in materials by atomistic computer simulations.[2] In addition to predicting diffusion coefficients, computer simulations can provide insights into atomic mechanisms of diffusion processes, creating a fundamental framework for materials design strategies through control of diffusion rates. In this paper we focus on the simplest case of self-diffusion in metals with the goal of testing different methods of diffusion calculations.

It is well established that self-diffusion in metals is mediated by migration of point defects. Under point-defect mechanisms, the diffusion coefficient D can be expressed by (Ref. 3)

$$D = a^2 f \gamma \nu x_e^d e^{-G_m^d/kT}, \tag{1}$$

where a is the jump length of atoms, γ is a geometrical factor, f is the jump correlation factor, ν is the attempt frequency which is on the order of typical frequencies of atomic vibrations, G_m^d is the free energy associated with the barrier of point-defect migration, kT is the thermal factor, and x_e^d is the equilibrium point-defect concentration. The latter is related to the point-defect formation free energy, G_f^d, by

$$x_e^d = e^{-G_f^d/kT}. \tag{2}$$

The free energy is divided into the energy and entropy parts by $G=E-TS$.

There is ample evidence that self-diffusion in face-centered cubic (fcc) metals is controlled by the vacancy mechanism. The self-interstitial formation energy in fcc metals is much larger than the vacancy-formation energy, making the interstitial contribution to diffusion negligibly small. The case of body-centered cubic (bcc) metals is more complex since the interstitial-formation energy can be only slightly higher than the vacancy-formation energy. Since the interstitial migration energy is usually very small, the activation energy of diffusion by the interstitial mechanism can be lower than that for the vacancy mechanism. For example, this conclusion was reached based on first-principles calculations for V.[4] Thus, in the case of bcc metals both mechanisms should be considered.

The most common approach to diffusion calculations is to compute all point-defect characteristics at $T=0$ K and then apply Eqs. (1) and (2) to obtain D. Because such calculations do not require large simulation cells, first-principles methods can be used to predict the diffusivity without any fitting parameters.[5] However, this approach relies on the assumption that all parameters in Eqs. (1) and (2) are temperature independent. Molecular dynamics (MD) simulations with semiempirical interatomic potentials indicate that this assumption is not realistic (see, e.g., Refs. 6–9): the defect-formation energies and other parameters do depend on temperature. This temperature dependence reflects the anharmonicity of atomic vibrations and other physical effects. Since it is not presently possible to compute diffusivities in solids directly from *ab initio* MD simulations, some temperature corrections must be introduced into the static methods. One possible way introduce such corrections is to use the quasiharmonic (QH) approximation to atomic vibrations, which will be discussed in Sec. III. However, the only way to test the accuracy of the QH approximation is to compare its predictions with either experiments (which are difficult and can be subject to the impurity effect and other sources of error) or more accurate and direct calculations.

Classical molecular dynamics simulations offer the most direct approach to diffusion calculations.[1] MD automatically captures the anharmonicity of atomic vibrations and all other sources of temperature effects. Unfortunately, lattice diffusion in solids is presently beyond the time scale accessible by MD simulations even with semiempirical potentials. The difficulties arise from at least three sources. One is that the

jump rates of point defects in crystals are very slow in comparison with typical jump rates in grain boundaries or at open surfaces. Second, in order to create and accurately compute the equilibrium point-defect concentration, the simulation block must contain sinks and sources of defects and thus have a large size. Third, after the simulation block reaches point-defect equilibrium, it contains a very small number of point defects, and producing statistically meaningful atomic displacements induced by those defects would require unrealistically long MD times. In this paper we demonstrate that some of these difficulties can be overcome by introducing several point defects in the simulation block, computing the diffusivity, and then making appropriate corrections for the equilibrium defect concentration.

Indeed, if several point defects are simultaneously present in the simulation block, the diffusion process is fast enough that the effective diffusivity D^{eff} per defect can be reliably computed from

$$D^{\mathrm{eff}} = D^{\mathrm{sim}}/x^{\mathrm{d}}. \tag{3}$$

Here, x^{d} is the actual point-defect concentration created in the simulation block,

$$D^{\mathrm{sim}} = \frac{\langle \Delta r^2 \rangle}{6t} \tag{4}$$

is the diffusivity obtained by the simulations, and $\langle \Delta r^2 \rangle$ is the mean-squared displacement of atoms during the simulation time t. The true diffusivity can be then calculated by

$$D = x_{\mathrm{e}}^{\mathrm{d}} D^{\mathrm{eff}} \tag{5}$$

knowing the equilibrium point-defect concentration $x_{\mathrm{e}}^{\mathrm{d}}$.

In order to calculate $x_{\mathrm{e}}^{\mathrm{d}}$, a separate simulation block containing some defect source (e.g., a grain boundary or free surface) must be used.[9,10] Reaching the equilibrium defect concentration requires long MD runs but can be implemented[9,10] as long as the temperature is high enough. At low temperatures this direct method becomes impractical, but then another approach can be used. The point-defect-formation energy can be readily computed by MD simulations as a function of temperature. The free energy of defect formation $G_{\mathrm{f}}^{\mathrm{d}}$ can be recovered by thermodynamic integration of this function and used to calculate the equilibrium defect concentration from Eq. (2).

The MD simulations give us the opportunity to test the QH approximation. Foiles[6] has extensively tested this approximation for calculations of free energies of crystalline defects, including a vacancy in Cu. However, because it was impossible at that time to compute the actual vacancy concentrations by direct MD simulations, Foiles tested his QH predictions against results of thermodynamic integration of the vacancy-formation energy.

In this paper we report on MD calculations of point-defect concentrations and self-diffusion coefficients in bcc Fe over a wide temperature range. We find that the simulation results are in good agreement with experimental data. We then compare the MD results for point-defect concentrations with QH calculations and conclude the QH approximation can give the correct order of magnitude but is far less accurate than MD.

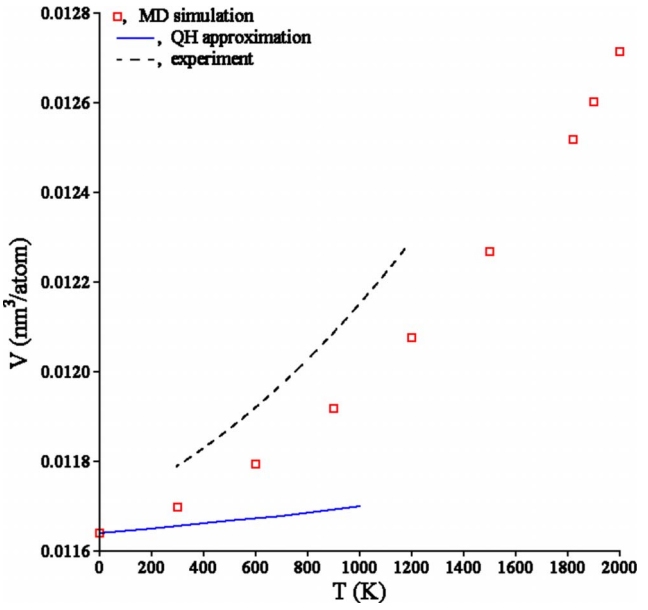

FIG. 1. (Color online) Equilibrium atomic volume of bcc Fe as a function of temperature obtained by MD simulations and in the QH approximation. The experimental thermal expansion (Ref. 12) is shown for comparison.

II. MOLECULAR DYNAMICS SIMULATION OF POINT DEFECTS AND SELF-DIFFUSION IN Fe

A. Atomic interactions and thermal expansion

The interatomic interactions in bcc Fe were modeled using the semiempirical interatomic potential developed in Ref. 11. This potential was fitted to zero-temperature *ab initio* data and the liquid density at the melting temperature T_{m}. Although the melting temperature was not included in the fitting procedure, the potential gives $T_{\mathrm{m}}=1795$ K in reasonable agreement with the experimental melting temperature of Fe (1812 K).

We started our study by calculating the equilibrium lattice parameter as a function of temperature. Simulation cells with 2,000 atoms and periodic boundary conditions were used. At a given temperature, *NVT* (constant number of atoms, volume, and temperature) MD simulations were run at several densities. After equilibration of the system by 20 000 MD steps (1 MD step=2 fs), statistics of pressure was collected during additional 20 000 steps. From an extrapolation of the pressure-volume relation to zero, the equilibrium atomic volume V vs temperature was found. The results are shown in Fig. 1 and can be described by the following interpolation formula:

$$V(\mathrm{nm}^3) = 11.64012 + 9.37798 \times 10^{-5} T + 3.643134 \times 10^{-7} T^2 - 1.851593 \times 10^{-10} T^3 + 5.669148 \times 10^{-14} T^4. \tag{6}$$

Figure 1 also shows experimental data.[12] The employed interatomic potential slightly underestimates the lattice parameter by 0.26% but provides correct thermal expansion coefficient.

B. Point-defect-formation energies

In order to determine the point-defect-formation energy we introduced a single point defect (vacancy or interstitial) in the simulation block and performed a 20 000-step MD run to equilibrate the model followed by additional 2 900 000 MD steps to compute its average energy E_d. A similar calculation was performed to compute the energy E_p of the same simulation block without any defects. The point-defect-formation energy E_f was determined as follows:

$$E_f = E_d - E_p N_d / N, \tag{7}$$

where N is the number of lattice sites in the simulation block ($N=2000$ in this simulation series), $N_d=N-1$ for a vacancy and $N_d=N+1$ for an interstitial. Since the simulation block had periodic boundary conditions in all directions and contained no point-defect sources, new defects could only form during the simulations by the formation of vacancy-interstitial pairs.

In order to estimate the statistical error of the determination of the point-defect-formation energies we performed eight independent MD simulations for the perfect lattice simulation cells containing a single point defect at $T=700$ and 1500 K. The simulation time was always 5.9 ns. The statistical error of the determination of the point-defect energies was estimated to be 0.5% at $T=700$ K and 1% at $T=1500$ K using 95% confidence intervals. In order to check if the MD step was small enough and did not affect the results, we also obtained the vacancy-formation energy at $T=1500$ K using the MD step of 1 fs and averaging over eight independent MD runs. This series of runs yielded 2.16 ± 0.02 eV while the series where MD step was 2 fs yielded 2.18 ± 0.03 eV. Therefore, we concluded that the MD step of 2 fs was small enough and used it in all subsequent simulations.

The obtained point-defect-formation energies are shown in Fig. 2. This figure reveals a very strong dependence of the defect-formation energy on temperature. In the temperature interval from 0 to ~1700 K, the vacancy-formation energy increases with temperature while the interstitial-formation energy decreases. At higher temperatures the vacancy-formation energy turns over and begins to decrease with temperature. This decrease was related in Ref. 9 to spontaneous formation of vacancy-interstitial pairs.

C. Effective diffusion coefficients

The same series of MD simulations was used to determine the effective diffusivities D^{eff} mediated by each of the two types of point defects. The effective diffusivities were computed from Eq. (3) and are shown in Fig. 3 in the Arrhenius coordinates. In order to determine the statistical error we used the same eight independent MD runs discussed in the previous section. The 95% confidence intervals are shown in

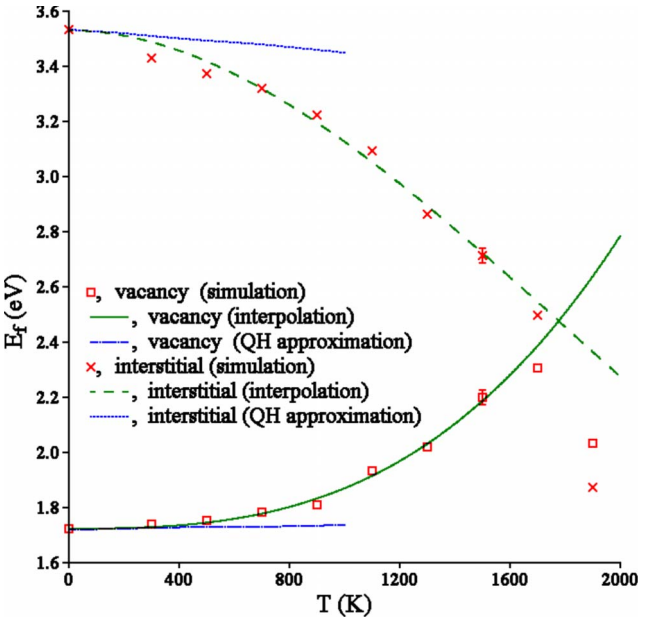

FIG. 2. (Color online) Point-defect-formation energies obtained by MD simulations and in the QH approximation as functions of temperature. The green curves show fits of the MD data by the interpolation formula (11).

Fig. 3. The data fall on straight lines up to ~1500 K. The linear fits give the defect migration energy E_m and the pre-exponential factor D_0^{eff} for each defect. The Arrhenius parameters obtained are given in Table I. At higher temperatures positive deviations from the straight lines are observed. These deviations are related to the spontaneous formation of vacancy-interstitial pairs, which increase the point-defect

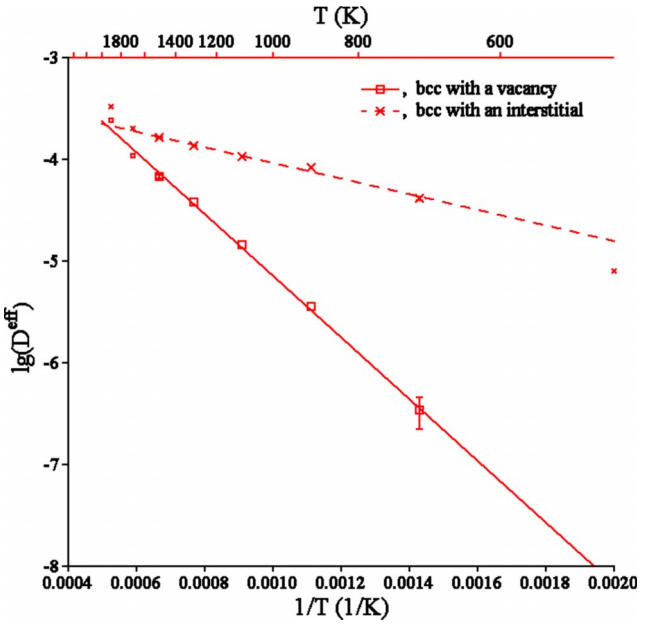

FIG. 3. (Color online) Arrhenius plot of the effective diffusivities by vacancies and interstitials obtained by MD simulations in bcc Fe. The lines show Arrhenius fits. The small symbols represent the data points which were not included in the Arrhenius fits for reasons explained in the text.

TABLE I. Arrhenius parameters of the effective diffusivity in bcc Fe obtained by MD simulations.

Defect	D_0^{eff} (cm^2/s)	E_m (eV)
Vacancy	7.87×10^{-3}	0.60
Interstitial	5.34×10^{-4}	0.15

concentration in the simulation block and thus enhance D^{sim}. The high-temperature points affected by the vacancy-interstitial pairs were excluded from the Arrhenius fits.

As expected, the migration energy by the interstitial mechanism is much smaller than that for the vacancy mechanism. It should be noted that at temperatures higher than 1500 K, the sum of the interstitial-formation and -migration energies (which gives the activation energy of diffusion by the interstitial mechanism) becomes smaller than a similar sum for the vacancy mechanism. Based on this observation, one might conclude that the diffusion process at high temperatures is dominated by the interstitial mechanism. However, we will see later that this is actually not the case.

D. Point-defect concentrations

Our MD data for the point-defect-formation energies (Fig. 2) are reliable only up to 1500 K. To compute point-defect concentrations at higher temperatures, more direct approaches must be applied. The MD simulations presented in Secs. II A–II C utilized simulation blocks with periodic boundary conditions in all directions. Such blocks are not suitable for direct calculations of equilibrium point-defect concentrations because new vacancies and interstitials can form in them only by pairs and their concentrations are bound to be equal. In real materials, vacancies and interstitials can be generated and eliminated by extended defects and their concentrations need not be equal.

This problem was solved by performing a new series of MD simulations, in which the simulation block had periodic boundary conditions only in the x and y directions and free surfaces in the z direction. The distance between the two free surfaces was ~185 Å. The surfaces served as sinks and sources of point defects. This simulation block contained 27 900 atoms and the MD time was ~41 ns (20 000 000 MD steps). This time was sufficient for the creation of equilibrium point-defect concentrations inside the block. The point defects were counted by identifying the lattice sites which either contained no atoms (vacancies) or contained two atoms (interstitials). Details of this procedure can be found elsewhere.[9]

In order to verify that the simulation time was sufficient for reaching the point-defect equilibrium, we performed an additional series of simulations in which 20 vacancies were introduced in the beginning of the simulation. After the equilibration, the same vacancy concentrations were found as in the simulations starting without any pre-existing vacancies, demonstrating that the equilibration time was long enough.

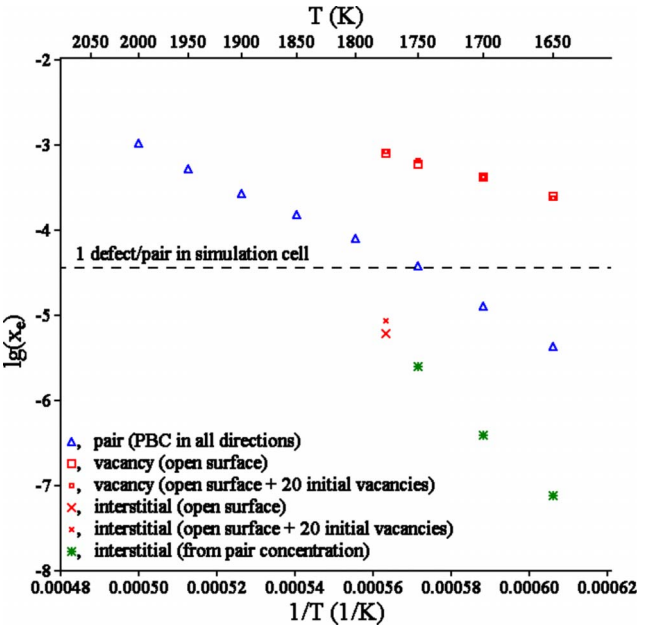

FIG. 4. (Color online) Arrhenius diagram of point-defect concentrations in bcc Fe obtained by MD simulations.

The obtained point-defect concentrations are shown in Fig. 4. The vacancy concentration is rather high reaching $\sim8\times10^{-4}$ at 1775 K, but the interstitial concentration is more than two orders of magnitude smaller. As a result, the simulation block contained only one or no interstitials at any given time, making the statistics of their concentration rather poor.

To determine the interstitial concentration more accurately, another series of simulations was performed using an all-periodic cell with 27 648 atoms. As mentioned earlier, vacancies and interstitials can now appear only by pairs and have the same concentration x_e^p. This concentration is related to the equilibrium vacancy and interstitial concentrations by

$$x_e^p = \sqrt{x_e^v x_e^i}, \tag{8}$$

which permits a calculation of x_e^i from x_e^p and x_e^v. Because the concentration of pairs is much higher than x_e^i, much better statistics could be obtained than in the simulations with open surfaces. Therefore, in the following calculations we will use the interstitial concentrations obtained from Eq. (8). Note that they are in good agreement with the open-surface calculation at 1775 K (Fig. 4).

E. Interpolation formulas for the point-defect properties

Summarizing the results of Secs. II B and II D we conclude that MD simulations give reliable data for point-defect-formation energies at relatively low temperatures until vacancy-interstitial pairs begin to form spontaneously during the simulations. On the other hand, reliable point-defect concentrations have been obtained at high temperatures where reasonable statistics of the defects can be collected. For diffusion calculations, we need to know the equilibrium point-

TABLE II. Coefficients in the interpolation expression for the free energy of point-defect formation [Eq. (9)].

Defect	g_0 (eV)	g_1 (eV/K)	g_2 (eV/K^2)	g_3 (eV/K^3)
Vacancy	1.724	-1.20×10^{-4}	-2.79×10^{-8}	-5.93×10^{-11}
Interstitial	3.530	-1.57×10^{-3}	$+4.94\times10^{-7}$	-4.51×10^{-11}

defect concentrations at all temperatures. We will obtain such concentrations by interpolation through all MD simulation data that we have so far.

To this end, we will assume that the free energy of point-defect formation can be represented by the following temperature dependence:

$$G_f = g_0 + g_1 T + g_2 T^2 + g_3 T^3 \tag{9}$$

with unknown coefficients g_k. It should be noted that the absolute free energy of a crystal contains a term $T \ln T$ arising from the classical expression for the vibrational free energy (Sec. III). However, G_f is a difference between free energies of the defected and perfect crystals having the same number of degrees of freedom. During the subtraction, the $T \ln T$ terms cancels out and we end up with a nonsingular expression. The point-defect-formation energy and free energy are related by the Gibbs-Helmholtz equation

$$\frac{\partial(G_f/T)}{\partial T} = -\frac{E_f}{T^2}, \tag{10}$$

which yields

$$E_f = g_0 - g_2 T^2 - 2g_3 T^3. \tag{11}$$

Finally, the formation entropy can be obtained from the standard relation $S_f = -\partial G_f / \partial T$, giving

$$S_f = -g_1 - 2g_2 T - 3g_3 T^2. \tag{12}$$

Note that g_0 and $-g_1$ have the meaning of the defect-formation energy and entropy, respectively, at 0 K.

The coefficients g_k have been determined by fitting to the MD data for the defect-formation energy at low temperatures and the defect concentrations x_e^d at high temperatures (recall that $G_f = -kT \ln x_e^d$). The coefficients obtained are listed in Table II. Figures 2 and 5 demonstrate that this interpolation provides a good agreement with the MD data for the formation energies of both defects at relatively low temperatures, and for the vacancy concentration at high temperatures. For interstitials, the interpolation gives the correct order of magnitude for the concentration at high temperatures (see Fig. 6).

The point-defect-formation entropy calculated from Eq. (12) is shown in Fig. 7. The vacancy-formation entropy increases with temperature while the interstitial-formation entropy decreases, which is consistent with the temperature dependences of the corresponding formation energies (cf. Fig. 2). The low-temperature value for the vacancy-formation entropy appears to be reasonable in comparison with other calculations.[5,13–15] The interstitial-formation entropy at low temperatures may look too high, but similarly high values were found in fcc Cu using the QH approximation[13] and MD simulation technique[10] similar to the method used in the present study. We also note that we did not examine the structural forms of the interstitials present in the simulated models at different temperatures. It is possible that the interstitials spontaneously switch between different dumbbell orientations or other structural forms, contributing to the entropy.

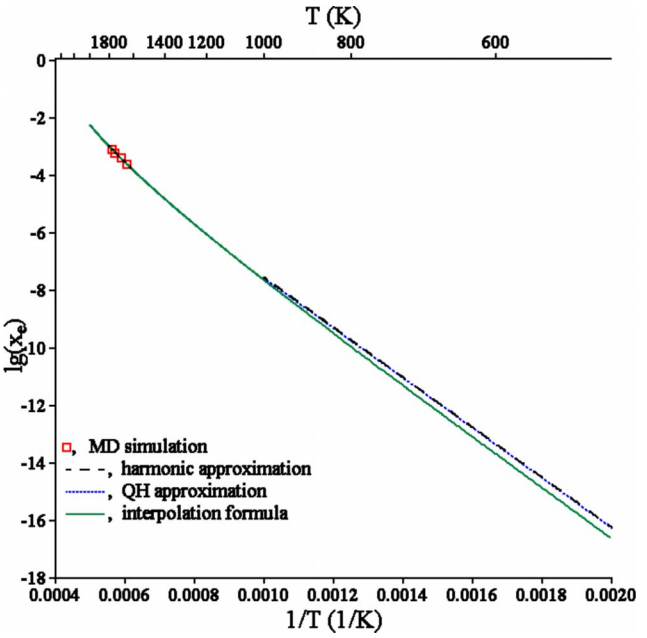

FIG. 5. (Color online) Arrhenius plot of the vacancy concentration in bcc Fe.

F. Self-diffusion coefficients

Finally, we can combine the effective diffusion coefficients with point-defect concentrations to determine the true

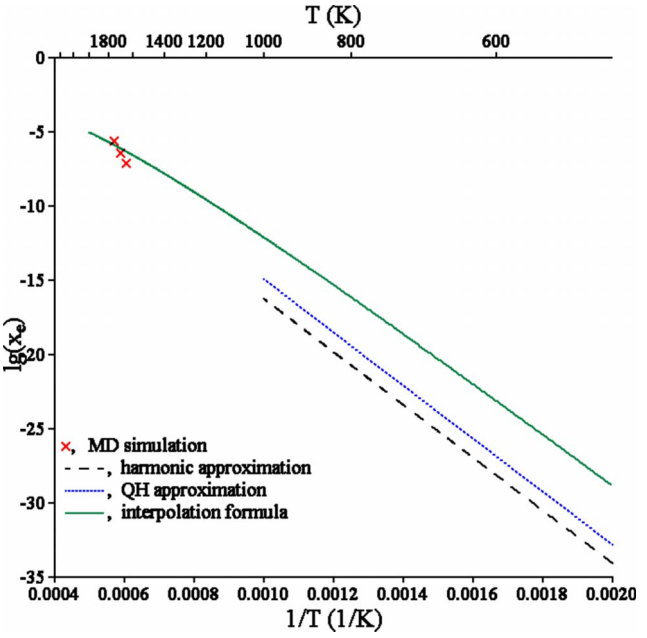

FIG. 6. (Color online) Arrhenius plot of the interstitial concentration in bcc Fe.

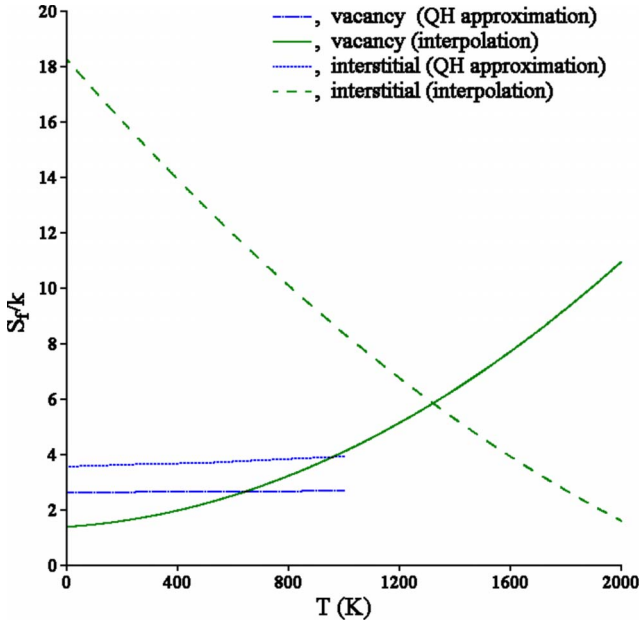

FIG. 7. (Color online) Calculated point-defect-formation entropy in bcc Fe as a function of temperature.

diffusion coefficients from Eq. (5). The results are presented in Fig. 8, which shows that self-diffusion in bcc Fe is dominated by the vacancy mechanism at all temperatures. At low temperatures this is due to the fact that the vacancy-formation energy is smaller than the interstitial-formation energy. At high temperatures the two formation energies become nearly equal, but the rapidly increasing vacancy-formation entropy combined with the rapidly decreasing interstitial-formation entropy keep the predominance of the vacancy mechanism.

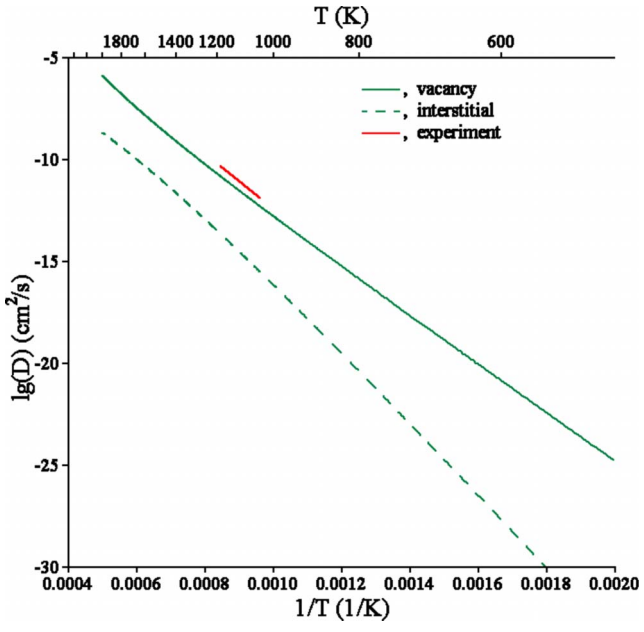

FIG. 8. (Color online) Arrhenius plot of calculated self-diffusion coefficients in bcc Fe by the vacancy and interstitial mechanisms in comparison with experimental data (Ref. 16).

Figure 8 also demonstrates that the simulation results are in reasonable agreement with experimental data.[16] This agreement confirms that the interatomic potential employed in this work is quite realistic and suitable for simulations of self-diffusion in bcc Fe.

III. HARMONIC AND QUASIHARMONIC CALCULATIONS

In the harmonic approximation, the potential energy of the equilibrium configuration is expanded into a Taylor series in atomic displacements and truncated at quadratic terms. The dynamical matrix is constructed and diagonalized to determine the normal vibrational frequencies of atomic vibrations.[6,13,17] If the boundary conditions are periodic in all directions, the dynamical matrix has three zero eigenvalues arising from the three translational degrees of freedom. These zeros are excluded from the harmonic calculation. Alternatively, one can fix the coordinates of one of the atoms and construct the dynamical matrix for all other atoms.

Knowing the normal frequencies ν_i, the vibrational part of the free energy can be calculated from the standard expression

$$F_{\mathrm{vib}} = kT \sum_{i=1}^{3(N-1)} \ln\left[2 \sinh\left(\frac{h\nu_i}{kT}\right)\right], \tag{13}$$

where $N-1$ is the number of dynamic atoms in the system. For small periodic cells, a summation over k points in the Brillouin zone must also be performed, but for large models such as those used in this work the direct summation in Eq. (13) already provides sufficient accuracy (Γ-point approximation). Using Eq. (13), the vibrational energy and entropy can be also calculated.

Equation (13) is based on the full quantum-mechanical treatment of atomic vibrations. In the context of comparison with classical MD simulations, we will use the classical limit of Eq. (13) at all temperatures, even though the classical approximation is physically inadequate at low temperatures. The classical expressions for vibrational free energy, energy, and entropy are

$$F_{\mathrm{vib}} = kT \sum_{i=1}^{3(N-1)} \ln\left(\frac{h\nu_i}{kT}\right), \tag{14}$$

$$E_{\mathrm{vib}} = 3(N-1)kT, \tag{15}$$

$$S_{\mathrm{vib}} = -k \sum_{i=1}^{3(N-1)} \ln\left(\frac{h\nu_i}{kT}\right) + 3(N-1)k. \tag{16}$$

For point-defect calculations, vibrational properties of simulation blocks with a single point defect and without any defects are compared for the same number of lattice sites N. This gives

$$S_f^v = -k \ln \frac{\prod_{i=1}^{3(N-2)} \nu_i}{\left(\prod_{i=1}^{3(N-1)} \nu_i^p\right)^{(N-2)/(N-1)}} \quad (17)$$

for the vacancy-formation entropy and

$$S_f^i = -k \ln \frac{\prod_{i=1}^{3N} \nu_i}{6\left(\prod_{i=1}^{3(N-1)} \nu_i^p\right)^{N/(N-1)}} \quad (18)$$

for the interstitial-formation entropy. Here, ν_i^p are normal frequencies in the perfect-lattice block with $N-1$ dynamic atoms. Factor 6 in the denominator accounts for six energetically equivalent orientations of the interstitial dumbbell.

Equation (15) shows that in the classical approximation, atomic vibrations do not contribute to the point-defect-formation energy explicitly [the $3(N-1)kT$ terms cancel out]. However, the anharmonicity of vibrations leads to thermal expansion of the lattice, which in turn can affect E_f^d. Likewise, temperature does not appear explicitly in the defect-formation entropy [Eqs. (17) and (18)]. Nevertheless, thermal expansion modifies the normal frequencies and affects S_f^d. In the harmonic approximation, the effect of thermal expansion is neglected and the point-defect free energy is taken in the form

$$G_f^d = E_f^d - TS_f^d, \quad (19)$$

using E_f^d and S_f^d computed at 0 K.

In the QH approximation,[6,13,17] the thermal expansion factor is computed by minimizing the total free energy of the perfect crystal, $E_p(V)+F_{vib}(T,V)$, with respect to atomic volume V at a given temperature T. The defect-formation energies and entropies are then computed as above, except that the perfect and defected simulation blocks equilibrated at 0 K are uniformly expanded by the QH thermal expansion factor prior to computing the normal frequencies. This gives E_f^d, S_f^d and thus G_f^d from Eq. (19) as functions of temperature. It should be emphasized that this calculation neglects the fact that lattice regions in the vicinity of the defect may have local thermal expansion factors somewhat different from the expansion factor of the perfect lattice. As a result, the atoms in the expanded configuration do not necessarily occupy the exact positions that would minimize the total free energy.

Both the harmonic and QH methods are applicable only at relatively low temperatures. At high temperatures, the amplitudes of atomic vibrations become so large that the quadratic expansion of energy adopted in both methods is no longer adequate. Furthermore, some atomic configurations can give negative eigenvalues of the dynamical matrix, indicating that the QH approximation is completely inadequate.

In this work, we used a 1024-atom periodic cell with a vacancy or interstitial created in its center with a fixed atom in one of the corners. Finite-size effects were estimated by testing larger cells and were found to be insignificant for the purposes of this work. Considering the limitations of the harmonic and QH methods mentioned above, they were applied only at temperatures from 0 to 1000 K.

Figure 1 demonstrates that the QH approximation significantly underestimates thermal expansion factors of bcc Fe in comparison with both MD simulations and experiments. This is already a sign that the temperature dependencies of point-defect characteristics will be underestimated.

Indeed, Figs. 2 and 7 show that the QH defect-formation energies and entropies vary with temperature much less rapidly than predicted by the MD simulations. The QH vacancy-formation entropy is in reasonable agreement with the MD calculations based on the interpolation formula. The harmonic and QH vacancy concentrations also compare reasonably well with the MD results at all temperatures. It should be noted that in the QH calculations of the vacancy concentration, there is apparently some compensation of errors at high temperatures, in which the underestimated formation energy is partially compensated by the underestimated entropy. The QH interstitial-formation entropy is drastically underestimated in comparison with the MD results. As a consequence, the interstitial concentration is a few orders of magnitude below the MD predictions.

IV. DISCUSSION AND CONCLUSIONS

In the present work we used the semiempirical potential for Fe (Ref. 11) to calculate the diffusivity in bcc Fe assuming two different mechanisms of self-diffusion: one mediated by migration of vacancies and the other mediated by migration of self-interstitials. No approximations besides the semiempirical potential were made in our calculations. We found that self-diffusion in bcc Fe is controlled by the vacancy mechanism at all temperatures. This result is due to the fact that the equilibrium vacancy concentration is always much larger than the equilibrium interstitial concentration, even though the vacancy-migration energy is much larger than the interstitial migration energy. It is interesting to note that the predominance of the equilibrium vacancy concentration over the interstitial concentration can be explained by the lower vacancy-formation energy only at low temperatures. At high temperatures, the interstitial- and vacancy-formation energies are about the same. However, the vacancy-formation entropy increases with temperature while the interstitial-formation entropy decreases. Thus, it is the high vacancy-formation entropy that is responsible for the larger vacancy concentration at high temperatures. The relationships between the point-defect properties at different temperatures established by our MD simulations are summarized in Table III.

The diffusivity of bcc Fe calculated for the vacancy mechanism is in good agreement with experimental data (note that under experimental conditions, the measured diffusivity can be enhanced by diffusion along grain boundaries and dislocations). This agreement confirms that the semiempirical potential employed in this work provides realistic predictions of vacancy properties of Fe. We are not aware of experimental data that could be compared with the MD results for interstitial properties. The potential well reproduces the interstitial-formation energy at $T=0$ obtained from *ab initio* calculations,[18] but this does not necessarily mean that it

TABLE III. Summary of point-defect properties and diffusion mechanisms in bcc Fe obtained by the MD simulations.

Temperature	Point-defect-formation energy	Point-defect-formation entropy	Point-defect concentration	Point-defect-migration energy	Diffusion mechanism
Low	$E_f^v < E_f^i$	$S_f^v < S_f^i$	$x_f^v > x_f^i$	$E_m^v > E_m^i$	vacancy
High	$E_f^v \approx E_f^i$	$S_f^v > S_f^i$	$x_f^v > x_f^i$	$E_m^v > E_m^i$	vacancy

can make reliable predictions at high temperatures. It would be interesting to perform similar simulations with another semiempirical potential for Fe to assess the sensitivity of the results to the interatomic potential.

Our finding, that self-diffusion in bcc Fe is mediated by vacancy migration, cannot be immediately generalized to all other bcc metals. In bcc Fe, the interstitial-formation energy at $T=0$ is much higher than the vacancy-formation energy, which need not be the case in all bcc metals. For example, *ab initio* calculations predict much closer vacancy- and interstitial-formation energies in bcc V.[4] It is possible that self-diffusion in some bcc metals can be dominated by interstitial migration. On the other hand, the results of the present study demonstrate that the activation energy calculated as the sum of the point-defect-formation and -migration energies (even if their temperature dependences are taken into account) is not sufficient for predicting the dominant diffusion mechanism. The entropy contribution can play a decisive role as has been demonstrated in this work.

The commonly used approximation is to neglect the temperature dependence of the point-defect-formation energy. Our MD simulations as well as previous studies[4,6–9] indicate that the temperature effect on defect-formation energies is rather significant. This effect is due to thermal expansion of the lattice and can be understood from the following simple considerations. The vacancy creates tensile stresses in surrounding crystal regions. The associated elastic strain energy constitutes a significant part of the vacancy-formation energy. Increasing the lattice parameter due to thermal expansion will increase the elastic strain energy and thus E_f^v. By the same reasoning, interstitials create a state of compression of the lattice and their energy could be expected to decrease with temperature. Figure 2 demonstrates these predictions hold for bcc Fe.

In reality, the situation with interstitials can be more complex. Their formation energy can also increase with temperature as was observed in MD simulations of V,[4] or can have a rather complicated temperature dependence as was found in bcc Zr.[9] This can be explained by the existence of multiple interstitial configurations with nearby energies. At low temperatures only the configuration with the lowest energy is implemented, but as temperature increases, other configurations are activated, changing the temperature dependence of the formation energy.

Molecular dynamics simulations of diffusion are computationally demanding even with atomistic potentials and are not presently feasible in conjunction with *ab initio* methods. In many cases, approximate methods such as harmonic or QH calculations are used. In this study, we found that the QH method gives reasonable results for vacancy properties in bcc Fe but performs poorly for interstitials. Some of these discrepancies can be attributed to specific features of the particular interatomic potential for Fe used in this work. These potential functions were defined by cubic splines, which are quite suitable for fitting to energies and forces but tend to be less predictable than analytical functions in capturing thermal expansion and other anharmonic effects. In the future, it would be interesting to examine if potentials based on analytical functions can give more accurate QH results.

Besides properties of particular potentials, there are generic limitations of the QH method that have contributed to the above discrepancies. Such limitations include the possible breakdown of the quadratic expansion of energy when vibrational amplitudes become large at high temperatures. They also include the neglect of the difference between the local thermal expansion around point defects and thermal expansion of the perfect lattice. Furthermore, the lattice distortions around defects can produce relatively shallow minima of the potential energy and can make the QH approximation less reliable than for perfect crystals even at relatively low temperatures. These limitations of the QH approximation can be more severe around interstitials, which produce much stronger lattice distortions than vacancies. In addition, part of the interstitial-formation entropy is due to the multiplicity of different orientations of the dumbbells and other structural forms of the interstitials at high temperatures. The harmonic and QH calculations were performed in this work for only the [110] dumbbell orientation. Even with these limitations, the QH approximation can give a better accuracy for point-defect concentrations than the simple harmonic method, see example in Fig. 6.

ACKNOWLEDGMENTS

Work at the Ames Laboratory was supported by the Department of Energy, Office of Basic Energy Sciences, under Contract No. DE-AC02-07CH11358. Y.M. was supported by NASA through Langley Research Center, NRA NNX08AC07A. Collaboration between the authors has greatly benefited from discussion during coordination meetings of Computational Materials Science Network (CMSN) program sponsored by DOE-BES.

*mendelev@ameslab.gov

[1] I. Kaur, Y. Mishin, and W. Gust, *Fundamentals of Grain and Interphase Boundary Diffusion* (John Wiley & Sons, Chichester, New York, 1995).
[2] Y. Mishin, in *Diffusion Processes in Advanced Technological Materials*, edited by D. Gupta (William Andrew, Norwich, NY, 2005), p. 113.
[3] P. G. Shewmon, *Diffusion in Solids* (McGraw-Hill, New York, 1963).
[4] M. I. Mendelev, S. W. Han, W. J. Son, G. J. Ackland, and D. J. Srolovitz, Phys. Rev. B **76**, 214105 (2007).
[5] M. Mantina, Y. Wang, R. Arroyave, L. Q. Chen, Z. K. Liu, and C. Wolverton, Phys. Rev. Lett. **100**, 215901 (2008).
[6] S. M. Foiles, Phys. Rev. B **49**, 14930 (1994).
[7] M. I. Mendelev and B. Bokstein, Mater. Lett. **61**, 2911 (2007).
[8] M. I. Mendelev, M. J. Kramer, C. A. Becker, and M. Asta, Philos. Mag. **88**, 1723 (2008).
[9] M. I. Mendelev and B. S. Bokstein, Philos. Mag. (to be published).
[10] K. Nordlund and R. S. Averback, Phys. Rev. Lett. **80**, 4201 (1998).
[11] G. J. Ackland, M. I. Mendelev, D. J. Srolovitz, S. Han, and A. V. Barashev, J. Phys.: Condens. Matter **16**, S2629 (2004).
[12] I. Seki and K. Nagata, ISIJ Int. **45**, 1789 (2005).
[13] Y. Mishin, M. R. Sorensen, and A. F. Voter, Philos. Mag. A **81**, 2591 (2001).
[14] S. B. Debiaggi, P. M. Decorte, and A. M. Monti, Phys. Status Solidi B **195**, 37 (1996).
[15] J. R. Fernandez, A. M. Monti, and R. C. Pasianot, Phys. Status Solidi B **219**, 245 (2000).
[16] M. Lubbehusen and H. Mehrer, Acta Metall. Mater. **38**, 283 (1990).
[17] J. M. Rickman and R. LeSar, Annu. Rev. Mater. Res. **32**, 195 (2002).
[18] C. Domain and C. S. Becquart, Phys. Rev. B **65**, 024103 (2001).